Prediction of vibration response of functionally graded sandwich plates by zig-zag theory

Simmi Gupta[*] and H.D. Chalak[a]

Department of Civil Engineering, National Institute of Technology, Kurukshetra, Haryana 136-119, India

(Received May 25, 2022, Revised November 6, 2022, Accepted November 7, 2022)

Abstract. This study is aimed to accurately predict the vibration response of two types of functionally graded sandwich plates, one with FGM core and another with FGM face sheets. The gradation in FGM layer is quantified by exponential method. An efficient zig-zag theory is used and the zigzag impacts are established via a linear unit Heaviside step function. The present theory fulfills interlaminar transverse stress continuity at the interface and zero condition at the top and bottom surfaces of the plate for transverse shear stresses. Nine-noded C-0 FE having 8DOF/node is utilized throughout analysis. The present model is free from the obligation of any penalty function or post-processing technique and hence is computationally efficient. Numerical results have been presented on the free vibration behavior of sandwich FGM for different end conditions, lamination schemes and layer orientations. The applicability of present model is confirmed by comparing with published results. Several new results are also specified, which will serve as the benchmark for future studies.

Keywords: finite element analysis; functionally graded material; sandwich plates; zig zag theory

1. Introduction

To withstand harsh environmental conditions, design requirement of incompatible properties like toughness and hardness, high melting point and strength, etc. at one place, generated a need of developing composite materials. Alloys have distinct material combinations, but alloying materials of different melting points is a difficult and impossible task (EI-Galy 2019). So, laminated composites (LC) which are a layer-by-layer combination of more than one material were developed. These were tested for thermo-mechanical loads and found to be good in withstanding stress conditions, having only drawback of material de-bounding at the interfaces (Garg and Chalak 2019). At the joining lamina, material properties were wide apart, so materials behaved differently (elongation) to the temperature elevation resulting in failure. To comply with stress failure at interfaces, functionally graded material (FGM) having a regular variation of material property was developed. The concept was applied firstly in 1984 for designing a thermal barrier in Japan (Koizumi 1997). FGM provides a way of controlling the material response by suitably choosing and varying material property. Different manufacturing methods of FGM are discussed by Owoputi (2018).

∗Corresponding author, Ph.D. Student, E-mail: simmi.nitk@gmail.com
[a]Ph.D.

Sandwich plates are a lower density material, so is very suitable to use in aerospace applications. It is a light weight option for the components of aircrafts components (Antony *et al.* 2019, Al-Fatlawi *et al.* 2021). FGM is used as a strong connecting layer between distinct material layers of sandwich plates to avoid delamination at interface. Functionally graded sandwich plates (FGSP) comprise layer(s) of FGM in between or at the edges of homogenous materials. Even when, FGM is superior to homogenous material, verified and reliable results are needed for generating confidence in the practical applications. Swaminathan *et al.* (2015), Garg *et al.* (2021) listed many theories developed by researchers to describe large stress variation of FGSP in thickness direction. Among all methods, elasticity theories provide most accurate results. Anderson (2003) presented 3D elasticity solutions for FGSP loaded transversally with rigid spherical indentor. Vel and Batra (2004) found vibration response of FGM plate using mori-tanaka and self-consistent methods for grading schemes. Woodward and Kashtalyan (2010) found 3D elasticity solutions for sandwich panels. Elasticity theories give benchmark data for comparison with simpler numerical methods.

Tounsi *et al.* (2016) used most basic Classical plate theory (CPT) which neglects transverse shear effects, so is useful for thin plates only. First-order shear deformation theory (FSDT) considers transverse shear effects, but fails to give stress free conditions at top and bottom of plate. Also, FSDT ignores transverse shear strains and is dependent on shear correction factor for getting acceptable results (Khalafi and Fazilati 2021) which in turn is dependent on various factors like: geometry, material property and boundary conditions. Ebrahimi (2014) used FSDT for analysing FGM shells. To alleviate the use of shear correction factor, many Higher-order shear deformation theories (HSDTs) are developed. Sahouane *et al.* (2019) presented dynamic analysis of FGM beam based on HSDT. Meksi *et al.* (2017) presented bending, buckling and vibration solutions of FGSP based on HSDT. Third-order shear deformation theory was employed by Reddy (2000) for analysis of FGSP. Third-order parabolic shear deformation theory is used by Ebrahimi and Barati (2017) for FGM nanobeams. Zenkour (2005a, 2005b) applied sinusoidal shear deformation theory for simply supported FGSP. Belabed *et al.* (2018) utilized hyperbolic shear deformation theory for analyzing FGSP. Benferhat *et al.* (2021), Nguyen *et al.* (2015) presented vibration response of FGSP using refined HSDT.

The displacement approximation in shear displacement theories can be based on central layer, assuming single layer construction: equivalent single layer (ESL) theory or individual layers: layer wise theory (LWT). ESL theory is simpler so, applied in most of the cases, but may not give acceptable results for multilayered plates and widely varied material properties in thickness direction. So, LWT and zig-zag theories (ZZT) were developed. Pandey and Pradyumna (2018), Moleiro *et al.* (2019), Hirane *et al.* (2021) utilized LWT for finding response of FGSP. LWT have advantage of realistic assumptions of DOF based on individual layers for multilayered plates, but becomes time consuming and non-economic with a hike in layers. Also LWT provides two values of shear stresses at joints of layers through two different approximations used for layers.

ZZT is ESL type, including an additional term (zig-zag factor, ZZF) to describe the kink/jump of the material properties at the interfaces of layers. A historic review on ZZTs is presented by Carrera (2003). As an alternate to expensive LWT, Murakami (1986) proposed a zig-zag factor to describe slope discontinuity. The advantages of using ZZT for multilayered plates and shells along with finite element implementation are discussed by Carrera (2004), Demasi (2008), Brischetto *et al.* (2009). FSDT based displacement approximation is used with ZZF by Shariyat and Alipour (2015) for analysing circular FGSP, hyperbolic shear deformation theory based displacements are used with ZZF by Neves *et al.* (2012) for analysing FGSP and sinusoidal shear deformation theory

based displacements are used with ZZF by Neves *et al.* (2017).

Engineering applications like automobiles, aircraft structures, ship hulls, submarine hulls, pipes carrying water and all such applications where high speed moving parts are used, require knowledge of vibration behavior. From the above discussion it can seen that different theories have been used by various researchers to analyze the FGM plate. The objective of the present paper is to utilize the most accurate theory for vibration behavior of the FG sandwich plates and present vibration results for inclined plates. An accurate theory should present the actual stress behavior of the plate at the interfaces of the two materials as well as at the top and bottom of plate. As it is known that the ESL theory assumes single layer architecture for the formulation of independent variables, which may not be accurate for analysis of multilayered plates. In literatures higher order terms have been used within ESL framework to increase the accuracy the results, which proved to be successful up to a certain limit, beyond which (at certain order of formulation) this advantage becomes insignificant. Some researchers found that LWT theories are more apt for analyzing sandwich plates than ESL theories, since LWT theory formulation uses layer-wise assumption of independent variables. But an increase in number of layers in plate design leads to larger number of equations to be solved making LWT complex an uneconomical. The unique feature of ZZT lies in realization of actual change of material property across the interface through zigzag term. The present ZZT fulfills all the requirements: stress free boundary conditions, single stress value at the interface and parabolic stress distribution of stress. The present theory uses ZZT and aims to provide accurate estimation of vibration response of the considered sandwich plates.

From the literature review, it is found that mostly analytical solutions were adopted by researchers for solving the independent variables for FGSP, which has restrictions in terms of geometry, boundary conditions, gradation of material properties and loading cases (Sharma *et al.* 2015, Chareonsuk and Vessakosol 2011). So, Finite element method (FEM), which is a numerical method, is adopted in this study for analyzing complex behaviour of FGSP. With an inclusion of zigzag factor in the independent variable assumption, the solution method on adoption of FEM becomes complex. To encounter zigzag factor C1 continuity issue rises. The problem of C1 continuity in using FEM for HSDT case is discussed by Chakrabarty *et al.* (2011). To alleviate C1 continuity Cho and Averill (2000) used sublaminate models; Averill (1994) used penalty functions and interpolation displacement; Di Sciuva (1985, 1993) used Hermitian functions to approximate transverse displacement. In this study HSDT is refined by expressing the differentiation variables of shear stress in terms of displacement terms to avoid C1 continuity. According to Li *et al.* (2016), the gradation of the FGM greatly determines analysis response, so is an important factor in analysis process. Most of the earlier studies use power law for material property quantification (Garg *et al.* 2021).

In present paper exponential law is used for obtaining free vibration response of FGSP through a higher-order zigzag theory. The zigzag impacts are established via a linear unit Heaviside step function. The present theory fulfills interlaminar transverse stress continuity at the interface and zero condition at the top and bottom surfaces of the plate for transverse shear stresses. Nine-noded C-0 FE having 8DOF/node is utilized throughout analysis. The present model is free from the obligation of any penalty function or post-processing technique and hence is computationally efficient. Free vibration behavior of FGSP made of exponential homogenization rule for various boundary conditions, orientation of layers and lamination schemes is determined. Present results are compared with those present in the literature to study the applicability of the proposed model. Several new results are also specified, which will serve as the benchmark for future studies.

Table 1 Material homogenization schemes

Nomenclature	Faces			$V_c(z)$			Figure
	Bottom	Core	Top	$z \in [h_0, h_1]$	$z \in [h_1, h_2]$	$z \in [h_2, h_3]$	
H-Type-E	FGM	Ceramic	FGM	$\left(\frac{2z+1}{2h_1+1}\right)^n$	1	$\left(\frac{2z-1}{2h_2-1}\right)^n$	5
S-Type-E	FGM	Metal	FGM	$1-\left(\frac{2z+1}{2h_1+1}\right)^n$	0	$1-\left(\frac{2z-1}{2h_2-1}\right)^n$	6
CT-Type-E1	Ceramic	FGM	Ceramic	1	$V_c(z) = \left(\frac{z-h_m}{h_1-h_m}\right)^n$ for $z \in [h_1, h_m]$ $\left(\frac{z-h_m}{h_2-h_m}\right)^n$ for $z \in [h_m, h_2], h_m = \frac{h_1+h_2}{2}$	1	7
MT-Type-E1	Metal	FGM	Metal	0	$1 - V_c(z)$ for CT-Type-E1	0	8

2. Homogenization rule

Two distinct forms of FGSP are examined which observe exponential law variation of material property across the thickness of plate:

Type E: Top and bottom face sheets comprise FGM. The central core comprises ceramic, then it is called as a hardcore-Type E plate (H-Type-E). If the central core comprises metal, then it is called as softcore-Type E (S-Type-E) sandwich plate (Fig. 1(a) &1(b)).

Type E1: the central core comprises FGM layer, If the top and bottom faces are made up of ceramic, then it is written as CT-Type E1, and if the top and bottom faces are made up of metal, then it is called as MT-Type E1 sandwich FGM plate (Fig. 2(a) &2(b)).

Table 1 quantifies the variation of volume fraction of ceramic phase, $V_c(z)$ in the thickness (z) direction for all four types of FGSP. Material property $P(z)$ is a function of material properties of metal (P_m), ceramic (P_c) and $V_c(z)$ given by Eq. (1).

$$P(z) = P_m \mathrm{e}^{\left(\ln\left(\frac{P_c}{P_m}\right)V_c(z)\right)} \tag{1}$$

3. Mathematical modeling

The in-plane displacement field is chosen as

$$U_{(x)} = u^{(0)} + z\varphi^{(x)} + z^2\mu^{(x)} + z^3\xi^{(x)} + z^4\psi^{(x)} + \sum_{i=1}^{N^{(u)}-1}\left(z - z_i^{(u)}\right)H\left(z - z_i^{(u)}\right)\Phi_i^{(x_u)} + \\ \sum_{j=1}^{N^{(l)}-1}\left(z - z_j^{(l)}\right)H\left(-z + z_j^{(l)}\right)\Phi_j^{(x_l)} \tag{2}$$

$$U_{(y)} = v^{(0)} + z\varphi^{(y)} + z^2\mu^{(y)} + z^3\xi^{(y)} + z^4\psi^{(y)} + \sum_{i=1}^{N^{(u)}-1}\left(z - z_i^{(u)}\right)H\left(z - z_i^{(u)}\right)\Phi_i^{(y_u)} + \\ \sum_{j=1}^{N^{(l)}-1}\left(z - z_j^{(l)}\right)H\left(-z + z_j^{(l)}\right)\Phi_j^{(y_l)} \tag{3}$$

The transverse displacement field is assumed as

$$U_{(z)} = l_1 w^{(u)} + l_2 w^{(0)} + l_3 w^{(l)} \text{ for core}$$
$$U_{(z)} = l_1 w^{(u)} \text{ for upper faces}$$
$$U_{(z)} = l_3 w^{(l)} \text{ for lower faces}$$

(4)

Where, $u^{(0)}, v^{(0)}$ are the displacement of any point on the mid-plane about *x*- and *y*-axis, $\varphi^{(x)}, \varphi^{(y)}$ are the rotation of the mid-plane about *y*-, *x*- respectively. $w^{(u)}, w^{(0)}$ and $w^{(l)}$ denote transverse displacement at upper, middle and bottom sheet of the core respectively and l_1, l_2, l_3 are the lagrangian interpolation factors in *z*-direction. $\mu^{(x)}, \mu^{(y)}, \xi^{(x)}, \xi^{(y)}, \psi^{(x)}, \psi^{(y)}$ represent higher-order unknowns. Φ denotes the slope of the $i^{\text{th}}/j^{\text{th}}$ layer for upper and lower layers. $H\left(z - z_i^{(u)}\right), H\left(z - z_i^{(u)}\right)$ represent the Heaviside unit step function. The above assumption is based on the formulation used by Chalak *et al.* (2013) with an advancement of including one fourth-order term in the in-plane displacement variables.

The stress-strain dependency for k^{th} layer can be expressed as

$$\{\sigma\} = [C]_{(k)}\{\varepsilon\}$$

(5)

where $\{\sigma\}, \{\varepsilon\}$ and $[C]$ are the stress, strain vector and compliance matrix for the kth layer, respectively. The matrix $[C]$ can written in same lines as given by Chalak *et al.* (2013).

Now utilizing conditions: Transverse stress-free condition at the top and bottom surface of the plate, Condition of transverse stress continuity at the interface and Additional conditions: $u = u^{(u)}, v = v^{(u)}, w = w^{(u)}$ at the top of the plate and $u = u^{(l)}, v = v^{(l)}, w = w^{(l)}$ at the bottom of the plate, the unknowns $\mu^{(x)}, \mu^{(y)}, \xi^{(x)}, \xi^{(y)}, \psi^{(x)}, \psi^{(y)}, \Phi_i^{[x^{(u)}]}, \Phi_j^{[x^{(l)}]}, \Phi_i^{[y^{(u)}]}, \Phi_j^{[y^{(l)}]}$, $\frac{\partial w^{(u)}}{\partial x}, \frac{\partial w^{(l)}}{\partial x}, \frac{\partial w^{(u)}}{\partial y}, \frac{\partial w^{(l)}}{\partial y}$ can be written in terms of displacements $u^{(0)}, v^{(0)}, \varphi^{(x)}, \varphi^{(y)}$, $u^{(u)}, v^{(u)}, u^{(l)}, v^{(l)}$ as

$$\{M\} = [N]\{\Theta\}$$

(6)

where, $\{\Theta\} = \left\{u^{(0)}, v^{(0)}, \varphi^{(x)}, \varphi^{(y)}, u^{(u)}, v^{(u)}, u^{(l)}, v^{(l)}\right\}^T$ and

$$\{M\} = \{\mu^{(x)}, \mu^{(y)}, \xi^{(x)}, \xi^{(y)}, \psi^{(x)}, \psi^{(y)}, \Phi_1^{[x^{(u)}]} \Phi_2^{[x^{(u)}]} \dots$$
$$\Phi_{N^{(u)}-1}^{[x^{(u)}]} \Phi_1^{[x^{(l)}]} \Phi_2^{[x^{(l)}]} \dots \Phi_{N^{(l)}-1}^{[x^{(l)}]} \Phi_1^{[y^{(u)}]} \Phi_2^{[y^{(u)}]} \dots$$
$$\Phi_{N^{(l)}-1}^{[y^{(l)}]}, \frac{\partial w^{(u)}}{\partial x}, \frac{\partial w^{(l)}}{\partial x} \frac{\partial w^{(u)}}{\partial y}, \frac{\partial w^{(l)}}{\partial y}\}^T$$

The elements of $[N]$ are dependent on the material property of the layer. Since the last four terms in the $\{M\}$ are the derivative terms and are denoted in terms of displacement components $\{\Theta\}$, hence the problem related with the C-1 continuity can be evaded simply by using the proposed model.

With the aid of Eq. (6), the Eqs. (2) and (3) can be re-arranged as

$$U_{(x)} = a^{(1)}u^{(0)} + a^{(2)}v^{(0)} + a^{(3)}\varphi^{(x)} + a^{(4)}\varphi^{(y)} + a^{(5)}u^{(u)} + a^{(6)}v^{(u)} + a^{(7)}u^{(l)} + a^{(8)}v^{(l)} \quad (7)$$

$$U_{(y)} = b^{(1)}u^{(0)} + b^{(2)}v^{(0)} + b^{(3)}\varphi^{(x)} + b^{(4)}\varphi^{(y)} + b^{(5)}u^{(u)} + b^{(6)}v^{(u)} + b^{(7)}u^{(l)} + b^{(8)}v^{(l)} \quad (8)$$

Here, the coefficients *a*'s, and *b*'s are dependent on the material properties, thickness coordinates, and the unit step function.

(a) H-Type E   (b) S-type E
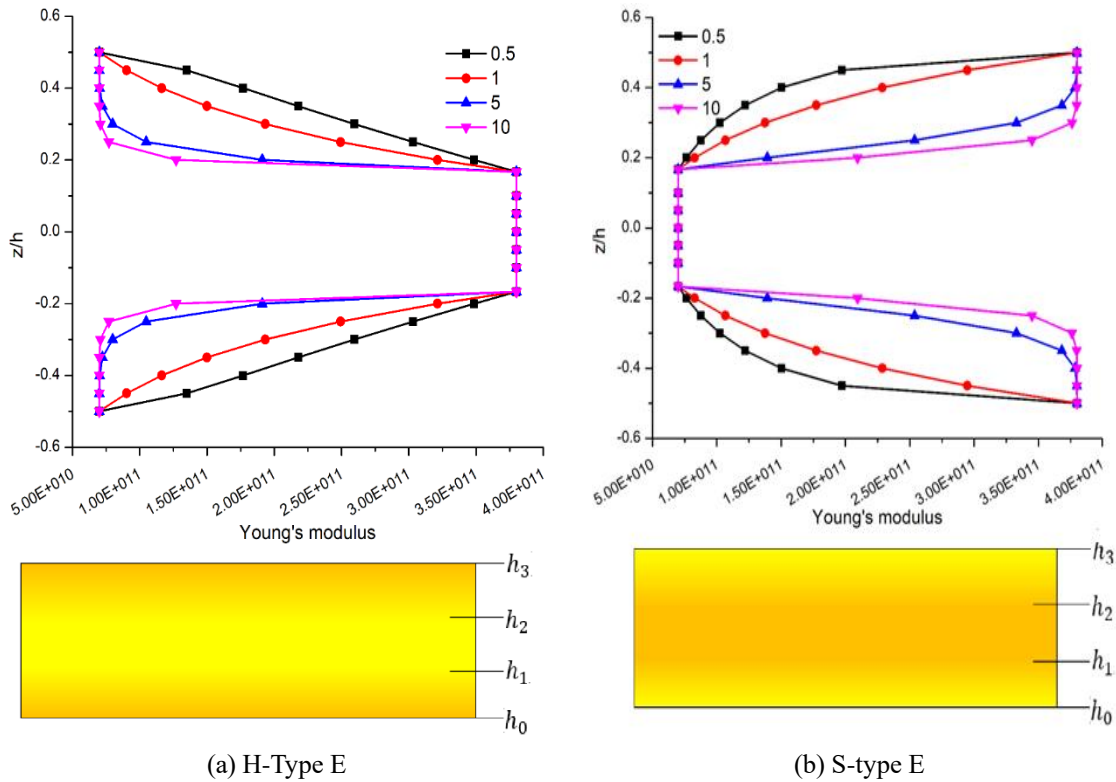
Fig. 1 Variation of Young's modulus and geometry across the thickness for 1-1-1 sandwich FGM plate

In the present work, nine-noded C-0 isoparametric FE having 8DOF/node is utilized. The connected DOF/node are $\{u^{(0)}, v^{(0)}, \varphi^{(x)}, \varphi^{(y)}, u^{(u)}, v^{(u)}, u^{(l)}, v^{(l)}\}$.

The generalised displacement for an element can be defined as

$$\{\delta\} = [N_i]\{\delta_i\} \tag{9}$$

where N_i is the shape function linked with the node.

Expressing strain-displacement dependency with the assistance of Eqs. (6-9), the strains can be expressed in the arrangement of unknowns as

$$\{\varepsilon\} = [B]\{\delta\} \tag{10}$$

where, $[B]$ is the strain-displacement affiliation on cartesian coordinates.

The governing equation of frequency can be derived on the same lines as done by Garg *et al.* (2022) from Hamilton's principle of the Equation of motion which can be written as

$$\int_0^t \delta(T - U)dt = 0 \tag{11}$$

where, T is kinetic energy $T = \frac{1}{2}\int \rho\left(\dot{U}_{(x)}^2 + \dot{U}_{(y)}^2 + \dot{U}_{(z)}^2\right)dv$ and $\dot{U}_{(x)}, \dot{U}_{(y)}$ and $\dot{U}_{(z)}$ are the derivatives of $U_{(x)}, U_{(y)}$ and $U_{(z)}$ respectively and ρ is the density of the material.

The potential energy of the plate is forces and damping also, Hamilton's principle principals to the equilibrium equation of a system, which can be quantified as

(a) CT-Type E1 (b) MT-Type E1
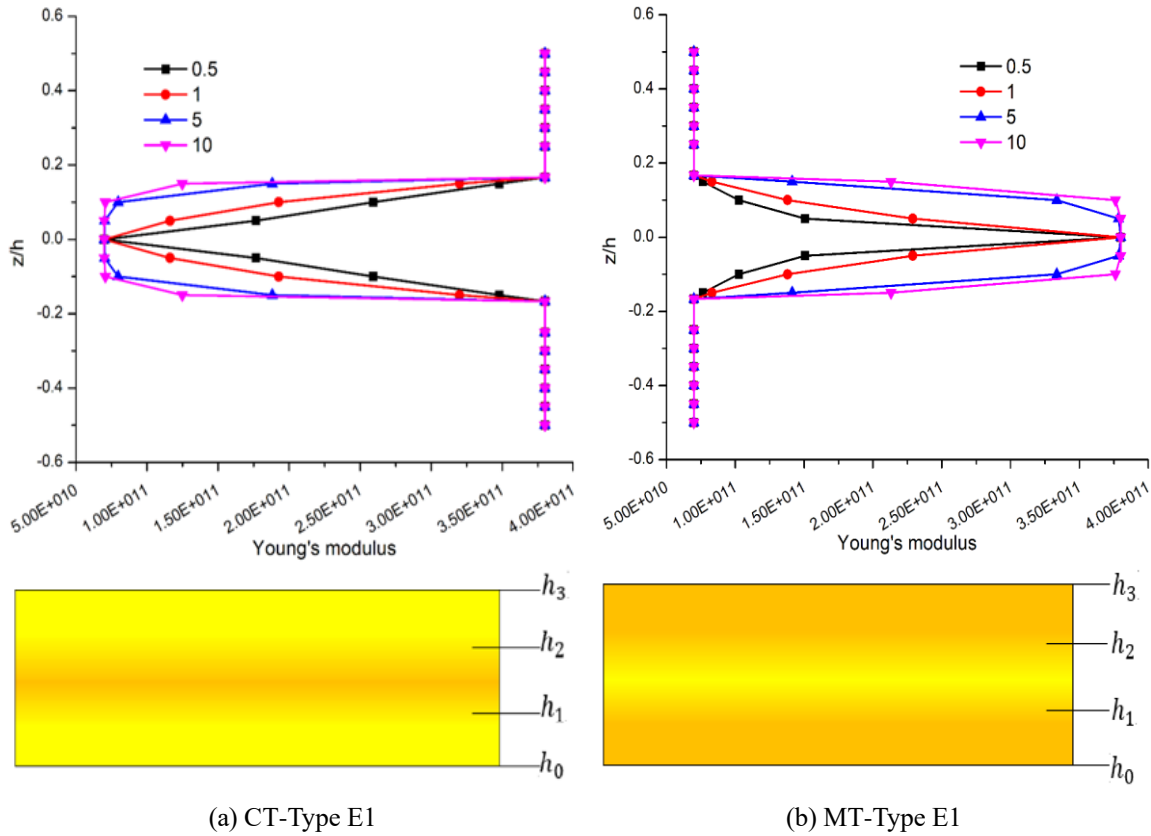
Fig. 2 Variation of Young's modulus and geometry across the thickness for 1-1-1 sandwich FGM plate

$$U = \frac{1}{2} \int \sigma_{xx}\varepsilon_{xx} + \sigma_{yy}\varepsilon_{yy} + \sigma_{zz}\varepsilon_{zz} + \sigma_{xz}\varepsilon_{xz} + \sigma_{yz}\varepsilon_{yz} + \sigma_{xy}\varepsilon_{xy} \, dv \tag{12}$$

or

$$U = \frac{1}{2}\sum_{k=1}^{n} \iiint \{\bar{\varepsilon}\}^T [C]\{\bar{\varepsilon}\} dx \, dy \, dz$$

Eq. (12) disregards external work done by external

$$[M]\left\{\frac{\partial^2 \bar{\delta}}{\partial t^2}\right\} + [K]\{\bar{\delta}\} = 0 \tag{13}$$

where, $[M], [K], \{\bar{\delta}\}, \left\{\frac{\partial^2 \bar{\delta}}{\partial t^2}\right\}$ are global mass matrix, stiffness matrix, nodal variable vector, and acceleration vector of the system respectively.

Frequency (λ) can be worked out utilizing Eq. (13)

$$[K]\{\bar{\delta}\} = \lambda^2 [M]\{\bar{\delta}\} \tag{14}$$

As elemental stiffness matrix $[K_e]$ is obtained on the same lines elemental mass matrix can be found out. Acceleration at any point within the plate can be expressed as

Table 2 Convergence and validation study for non-dimensional natural frequency ($\bar{\lambda}$)

Boundary condition	Source	Non-dimensional natural frequency
CCCC	Present (4×4)	39.9482
	Present (8×8)	32.2883
	Present (10×10)	29.5326
	Present (16×16)	28.6871
	Present (20×20)	28.6871
	Chakraverty and Pradha (2014)	28.3422
CSCS	Present (4×4)	35.5630
	Present (8×8)	28.8051
	Present (10×10)	24.2697
	Present (16×16)	23.0815
	Present (20×20)	23.0815
	Chakraverty and Pradha (2014)	22.7996
SSSS	Present (4×4)	26.6256
	Present (8×8)	20.7355
	Present (10×10)	17.0531
	Present (16×16)	15.9862
	Present (20×20)	15.9862
	Chakraverty and Pradha (2014)	15.5462

$$\left\{ \frac{\partial^2 \bar{\delta}}{\partial t^2} \right\} = \left\{ \begin{array}{c} \frac{\partial^2 \bar{U}_{(x)}}{\partial t^2} \\ \frac{\partial^2 \bar{U}_{(y)}}{\partial t^2} \\ \frac{\partial^2 \bar{U}_{(w)}}{\partial t^2} \end{array} \right\} = -\lambda^2 \left\{ \begin{array}{c} U_{(x)} \\ U_{(y)} \\ U_{(z)} \end{array} \right\} = -\lambda^2 [\Delta]\{\delta\} \tag{15}$$

where, $[\Delta]$ is holding terms of z and some constant values.

$$[M] = \sum_{i=1}^{N^{(u)}+N^{(l)}} \int \rho_i [N]^T [\Delta]^T [N][\Delta] dx\, dy\, dz = \int [N]^T [L][N] dx\, dy\, dz \tag{16}$$

where, ρ_i is the mass matrix of the i-th layer.

$[L]$ appeared in the above equation can be inscribed as

$$L = \sum_{i=1}^{N^{(u)}+N^{(l)}} \int \rho_i [\Delta]^T [\Delta] dx \tag{17}$$

The skyline storage technique is utilized to stock the global stiffness matrix in a single array, and after that simultaneous iteration technique is utilized for resolving the governing equations. The above conversed FE-based model is scripted in FORTRAN for finding the frequency for FGSP. The free vibration response is determined for the four types of FGSP governed by exponential homogenization rule, as discussed above. Following six different thickness patterns are employed for the study: 1-1-1, 1-2-1, 2-1-2, 2-2-1, 2-1-1 and 1-8-1. 2-1-1 characterizes the

Table 3 Variation of non-dimensional natural frequency for SSSS square-shaped Type-E sandwich FGM plate

a/h	n	2-1-2	2-1-1	1-1-1	2-2-1	1-2-1	1-8-1
				H-Type-E			
100	0.5	1.3748	1.4391	1.4190	1.4850	1.4861	1.7111
	1	0.9219	1.2851	1.2260	1.3439	1.3612	1.6454
	5	1.0245	1.0476	1.0349	1.1320	1.1413	1.5473
	10	0.9976	0.6499	1.0145	1.1178	1.0415	1.5366
10	0.5	1.3013	1.3720	1.3828	1.4269	1.4775	1.6619
	1	0.9080	1.2146	1.2288	1.2827	1.3398	1.6005
	5	1.0002	1.0223	1.0010	1.1070	1.1204	1.5083
	10	0.9092	0.9109	0.9976	1.1216	1.0848	1.4982
				S-Type-S			
100	0.5	1.6325	1.6266	1.6118	1.5978	1.4732	1.3021
	1	1.7819	1.7663	1.7531	1.6263	1.5951	1.3919
	5	1.8967	1.9773	1.9945	1.8603	1.9524	1.6243
	10	2.0075	1.9907	2.0177	1.8865	1.9906	1.6692
10	0.5	1.4080	1.5047	1.4864	1.3758	1.4515	1.1240
	1	1.5352	1.6252	1.6025	1.4826	1.5498	1.2599
	5	1.8237	1.8192	1.7940	1.7701	1.7440	1.4980
	10	1.8369	1.8456	1.8118	1.7899	1.7692	1.5824

bottom, and core faces are of the same thickness, and the top face has a thickness twice as that of the core. Following is the relationship used to convert the natural frequency into non-dimensional form ($\bar{\lambda}$)

$$\bar{\lambda} = \lambda a^2 \sqrt{\frac{\rho_c h}{D_c}}; \ D_c = \frac{h^3 E_c}{12(1 - v^2)} \tag{18}$$

4. Result and discussions

4.1 Convergence study

For choosing the appropriate mesh size for the analysis of exponentially graded sandwich FGM plate, convergence study is carried out at first. Material properties used during the present study are: Metallic phase is made up of Aluminium (Al) $E = 70$ GPa, $v = 0.30, \rho = 2707$ kg/m^3.

The ceramic phase is made up of Alumina (Al_2O_3) $E = 380$ GPa, $v = 0.30, \rho = 3800$ kg/m^3. The results for the convergence study are reported in Table 1 for different end conditions. It can be observed that the present results converge at the mesh size of 16 x 16. Therefore, in further studies, same mesh size is adopted. Present results are compared with the Rayleigh-Ritz method-based CPT given by Chakraverty and Pradha (2014). Some discrepancy in the results is observed due to the adoption of CPT.

Simmi Gupta and H.D. Chalak

Table 4 Variation of non-dimensional natural frequency for Type-E square shaped (*a/h*=4) sandwich FGM plate with different end conditions

Thickness scheme	*n*	CCCC	SSCC	CCCF	CCFF	SSSS	CFFF
				H-Type-E			
2-1-2	0.5	1.8452	1.5462	1.2845	1.2234	1.2031	0.2329
	1	1.4765	1.1396	1.1364	1.1042	0.8458	0.2054
	5	1.3858	1.1600	0.9629	0.9170	0.8998	0.1734
	10	1.3472	1.1369	0.9322	0.8857	0.8954	0.1707
2-1-1	0.5	1.8886	1.5934	1.3051	1.2399	1.2506	0.2371
	1	1.7317	1.4577	1.1888	1.1285	1.1285	0.2121
	5	1.4188	1.1821	0.9956	0.9493	0.9189	0.1807
	10	1.1135	0.7939	0.9403	0.9253	0.6007	0.1766
1-1-1	0.5	1.9182	1.6150	1.3276	1.2620	1.2639	0.2403
	1	1.7530	1.4625	1.2165	1.1576	1.1239	0.2156
	5	1.4086	1.1308	1.0246	0.9837	0.8394	0.1808
	10	1.4037	1.1485	0.9990	0.9550	0.8644	0.1771
2-2-1	0.5	1.9513	1.6457	1.3510	1.2830	1.2915	0.2454
	1	1.8163	1.5267	1.2517	1.1881	1.1829	0.2228
	5	1.5640	1.3062	1.0821	1.0276	1.0034	0.1907
	10	1.5269	1.2782	1.0550	1.0010	0.9844	0.1872
1-2-1	0.5	1.9931	1.6808	1.3819	1.3120	1.3193	0.2512
	1	1.8731	1.5728	1.2948	1.2289	1.2183	0.2304
	5	1.6418	1.3601	1.1453	1.0877	1.0295	0.1990
	10	1.5635	1.2726	1.1181	1.0666	0.9510	0.1950
1-8-1	0.5	2.1772	1.8440	1.5274	1.4462	1.4661	0.2853
	1	2.1255	1.7966	1.4899	1.4101	1.4196	0.2753
	5	2.0450	1.7233	1.4321	1.3541	1.3486	0.2604
	10	2.0359	1.7151	1.4256	1.3479	1.3409	0.2588

4.2 Vibration analysis

Type-E sandwich FGM plate: The results for non-dimensional natural frequencies, $\bar{\lambda}$ for Type-E plate are entirely new in the present work and are presented in Table 3. With increase in value of *a/h*, value of $\bar{\lambda}$ decreases for both H-Type-E and S-Type-E plates. With increase in value of n, value of $\bar{\lambda}$ decreases for H-Type-E plate and increases for S-Type-E plate. With increase in thickness of core, value of $\bar{\lambda}$ increases for H-Type-E plate and decreases for S-Type-E plate. When thickness of core is less, H-type-E plates exhibit less stiff behavior as compared to corresponding S-Type-E plates. But when thickness of core increases, H-Type-E plate shows stiffer behavior as compared to corresponding S-Type-E plate. Table 4 shows the value of $\bar{\lambda}$ for Type-E plate (*a/h*=4) with different end conditions. The boundary conditions, along with the thickness schemes, affect the vibration response of the plate.

Type-E1 sandwich FGM plate: Results for $\bar{\lambda}$ for Type-E1 plate are reported in Table 5. The CT-Type-E1 plate shows a considerable value of $\bar{\lambda}$ as compared to corresponding MT-Type-E1 plates. For plates with symmetric thickness schemes, $\bar{\lambda}$ is almost two times the non-dimensional natural frequency of the MT-Type-E1 plate. For unsymmetric plates, the same is found to be approximately 1.7 times of MT-Type-E1 plate. For the thin Type-E1 plate, the value of $\bar{\lambda}$ increases

Table 4 Continued

		S-Type-E					
2-1-2	0.5	1.6081	1.4165	1.2376	1.1609	1.0962	0.2696
	1	1.7051	1.5040	1.3155	1.2335	1.1636	0.2913
	5	1.9065	1.6737	1.4478	1.3750	1.2963	0.3236
	10	1.9476	1.7047	1.4675	1.4012	1.3215	0.3261
2-1-1	0.5	1.6061	1.4165	1.2389	1.1538	1.0880	0.2660
	1	1.7039	1.5052	1.3158	1.2228	1.1514	0.2854
	5	1.9318	1.7014	1.4666	1.3761	1.2953	0.3180
	10	2.0143	1.7678	1.5130	1.4310	1.3491	0.3235
1-1-1	0.5	1.5699	1.3856	1.2155	1.1344	1.0706	0.2653
	1	1.6412	1.4525	1.2786	1.1897	1.1212	0.2849
	5	1.7739	1.5704	1.3784	1.2875	1.2105	0.3169
	10	1.7978	1.5888	1.3892	1.3031	1.2251	0.3200
2-2-1	0.5	1.5627	1.3801	1.2119	1.1248	1.0604	0.2611
	1	1.6319	1.4452	1.2720	1.1752	1.1060	0.2779
	5	1.7652	1.5663	1.3725	1.2680	1.1898	0.3079
	10	1.7885	1.5849	1.3835	1.2827	1.2033	0.3112
1-2-1	0.5	1.5291	1.3514	1.1897	1.1052	1.0427	0.2588
	1	1.5766	1.3988	1.2383	1.1440	1.0779	0.2753
	5	1.6578	1.4798	1.3189	1.2102	1.1360	0.3069
	10	1.6672	1.4881	1.3252	1.2173	1.1419	0.3108
1-8-1	0.5	1.4149	1.2363	1.0659	1.0134	0.9582	0.2220
	1	1.4452	1.2697	1.1068	1.0395	0.9818	0.2341
	5	1.5015	1.3374	1.1950	1.0917	1.0275	0.2639
	10	1.5078	1.3466	1.2083	1.0985	1.0331	0.2693

Table 5 Variation of non-dimensional natural frequency for SSSS square-shaped Type-E1 sandwich FGM plate

a/h	n	2-1-2	2-1-1	1-1-1	2-2-1	1-2-1	1-8-1
		CT-Type-E1					
100	0.5	2.0948	1.6947	2.0945	1.4218	2.0875	2.0169
	1	2.1070	1.7909	2.1040	1.5807	2.0937	1.9767
	5	2.1432	1.8252	2.1327	2.0969	2.1203	1.8605
	10	2.1443	1.8247	2.1459	2.0960	2.1342	1.8314
10	0.5	1.9607	1.6375	1.9537	1.3802	1.9412	1.8756
	1	1.9653	1.7207	1.9493	1.5118	1.9285	1.8234
	5	1.9705	1.7388	1.9343	1.9073	1.9134	1.6987
	10	1.9689	1.7364	1.9382	1.8961	1.9038	1.6717
		MT-Type-E1					
100	0.5	1.0344	1.0354	1.0356	1.0238	1.0496	1.0806
	1	1.0361	1.0325	1.0409	1.0769	1.0659	1.2250
	5	1.0395	1.0348	1.0593	1.1172	1.0900	1.4566
	10	1.0397	1.0360	1.0622	1.1403	1.1698	1.5733
10	0.5	1.0012	0.9982	1.0049	0.9911	1.0211	1.0540
	1	1.0038	0.9958	1.0120	1.0441	1.0519	1.2135
	5	1.0086	0.9984	1.0147	1.0880	1.0740	1.4201
	10	1.0090	0.9995	1.0366	1.1108	1.1455	1.5300

Table 6 Variation of non-dimensional natural frequency for Type-E1 square shaped (a/h=4) sandwich FGM plate with different end conditions

Thickness scheme	n	CCCC	SSCC	CCCF	CCFF	SSSS	CFFF
				CT-Type-E1			
	0.5	2.1021	1.8258	1.5019	1.4207	1.5489	0.3309
2-1-2	1	2.0774	1.8080	1.4849	1.4035	1.5395	0.3304
	5	1.9890	1.7398	1.4231	1.3408	1.4945	0.3271
	10	1.9811	1.7333	1.4177	1.3354	1.4894	0.3268
	0.5	2.1800	1.8506	1.5638	1.5007	1.4204	0.3294
2-1-1	1	2.1835	1.8855	1.5306	1.4595	1.4659	0.3272
	5	2.1152	1.8551	1.4512	1.3753	1.4471	0.3222
	10	2.1049	1.8492	1.4408	1.3645	1.4413	0.3214
	0.5	2.0608	1.7941	1.4767	1.3963	1.5295	0.3302
1-1-1	1	2.0033	1.7500	1.4390	1.3590	1.5009	0.3287
	5	1.8610	1.6383	1.3432	1.2635	1.4222	0.3231
	10	1.8404	1.6227	1.3285	1.2485	1.4129	0.3222
	0.5	1.9307	1.5919	1.4776	1.4384	1.2206	0.3269
2-2-1	1	1.8903	1.5921	1.4267	1.3781	1.2759	0.3240
	5	1.8404	1.6228	1.3205	1.2410	1.4107	0.3147
	10	1.8031	1.5909	1.2978	1.2191	1.3870	0.3129
	0.5	2.0105	1.7559	1.4444	1.3650	1.5065	0.3277
1-2-1	1	1.9223	1.6881	1.3865	1.3079	1.4624	0.3244
	5	1.7323	1.5404	1.2594	1.1819	1.3632	0.3154
	10	1.6961	1.5124	1.2347	1.1572	1.3456	0.3133
	0.5	1.9263	1.6861	1.3865	1.3103	1.4539	0.3165
1-8-1	1	1.8016	1.5870	1.3026	1.2290	1.3843	0.3066
	5	1.5788	1.4068	1.1489	1.0809	1.2547	0.2820
	10	1.5394	1.3747	1.1208	1.0539	1.2328	0.2760
				MT-Type-E1			
	0.5	1.2776	1.0849	0.8724	0.8919	0.8480	0.1695
2-1-2	1	1.2920	1.0961	0.8779	0.8995	0.8550	0.1696
	5	1.3193	1.1166	0.8873	0.9147	0.8692	0.1701
	10	1.3211	1.1180	0.8879	0.9158	0.8702	0.1702
	0.5	1.2456	1.0542	0.8582	0.8863	0.8445	0.1732
2-1-1	1	1.2529	1.0551	0.8576	0.8962	0.8548	0.1744
	5	1.2712	1.0620	0.8617	0.9161	0.8750	0.1770
	10	1.2741	1.0636	0.8628	0.9187	0.8778	0.1774

with an increase in n for both types. But for the plate with a/h=10, the value of $\bar{\lambda}$ decreases with an increase in the value of n for symmetric thickness schemes and increases for unsymmetric thickness schemes for CT-Type-E plates. But for MT-Type-E1 plates, $\bar{\lambda}$ increases with an increase in the value of n.

Table 6 shows variation of $\bar{\lambda}$ for Type-E1 plate (a/h=4) with different end conditions. For thick plate, the $\bar{\lambda}$ decreases with an increase in the value of n for all types of thickness schemes and end conditions for the CT-Type-E1 plate. The opposite behavior is observed for the MT-Type-E1 plate. Among Type-E, and E1 plates, the CT-Type-E1 plate gives the maximum value of $\bar{\lambda}$, and the MT-Type-E1 plate gives the least value of $\bar{\lambda}$.

Table 6 Continued

1-1-1	0.5	1.3107	1.1095	0.8837	0.9113	0.8665	0.1701
	1	1.3638	1.1674	0.8965	0.9447	0.8911	0.1725
	5	1.4104	1.1811	0.9135	0.9749	0.9275	0.1748
	10	1.4335	1.2029	0.9318	0.9863	0.9375	0.1761
2-2-1	0.5	1.2830	1.0756	0.8644	0.9149	0.8738	0.1747
	1	1.3603	1.1492	0.9161	0.9471	0.9007	0.1765
	5	1.4873	1.2482	0.9715	1.0261	0.9754	0.1848
	10	1.5230	1.2790	0.9931	1.0476	0.9952	0.1880
1-2-1	0.5	1.3606	1.1490	0.9065	0.9411	0.8948	0.1724
	1	1.4075	1.1775	0.9121	0.9772	0.9310	0.1754
	5	1.5037	1.2150	0.9633	1.0795	1.0356	0.1902
	10	1.6316	1.3622	1.0425	1.1226	1.0677	0.1969
1-8-1	0.5	1.4418	1.2105	0.9445	1.0009	0.9533	0.1814
	1	1.6512	1.4274	0.9615	1.0575	1.0311	0.1917
	5	1.9259	1.6226	1.2699	1.3291	1.2635	0.2401
	10	2.0262	1.7131	1.3553	1.4034	1.3339	0.2582

Table 7 Non-dimensional natural frequency for SSSS Type-E rhombic plate (*a/h*=10)

Ξ^0	*n*	2-1-2	2-1-1	1-1-1	2-2-1	1-2-1	1-8-1
				H-Type-E			
15°	0.5	1.4176	1.4802	1.4918	1.5277	1.5598	1.7542
	1	0.9667	1.3255	1.3094	1.3862	1.4253	1.6895
	5	1.0561	1.0790	0.9561	1.1687	1.1848	1.5923
	10	1.0653	0.6705	0.9929	1.1523	1.0861	1.5818
30°	0.5	1.6873	1.7579	1.7722	1.8141	1.8522	2.0816
	1	1.1640	1.5768	1.5591	1.6474	1.6935	2.0054
	5	1.2548	1.2797	1.1470	1.3876	1.4125	1.8909
	10	1.1080	0.7764	1.1869	1.3682	1.3000	1.8784
45°	0.5	2.3364	2.4301	2.4504	2.5074	2.5600	2.8732
	1	1.6099	2.1853	2.1612	2.2805	2.3439	2.2700
	5	1.7343	1.7638	1.5944	1.9186	1.9614	2.6145
	10	0.7890	1.0317	1.6483	1.8914	1.8073	2.5975
60°	0.5	4.1037	4.2661	4.3047	4.3961	4.4952	4.6760
	1	2.4453	3.8530	3.8096	4.0194	4.1308	4.6540
	5	2.2949	3.0858	2.7997	3.3801	3.4694	4.5980
	10	0.6059	1.4889	2.9009	3.3294	2.9566	4.5697
				S-Type-E			
15°	0.5	1.6944	1.6907	1.6712	1.6599	1.6343	1.3955
	1	1.8281	1.8177	1.7932	1.7721	1.7374	1.4750
	5	2.0264	2.0224	1.9935	1.9687	1.9400	1.6718
	10	2.0404	2.0511	2.0121	1.9892	1.9661	1.7078
30°	0.5	1.9969	1.9927	1.9686	1.9554	1.9247	1.6476
	1	2.1527	2.1416	2.1098	2.0860	2.0436	1.7397
	5	2.3846	2.3840	2.3401	2.3130	2.2743	1.9659
	10	2.4017	2.4208	2.3614	2.3363	2.3031	2.0067

Table 7 Continued

45°	0.5	2.7068	2.7037	2.6666	2.6511	2.6071	2.2469
	1	2.9112	2.9020	2.8492	2.8221	2.7595	2.3666
	5	3.2196	3.2323	3.1431	3.1153	3.0473	2.6554
	10	3.2448	3.2908	3.1703	3.1446	3.0810	2.7065
60°	0.5	3.0926	3.1847	3.0975	3.1458	3.0769	2.7960
	1	3.2742	3.4011	3.2714	3.3405	3.2330	2.8932
	5	3.6770	3.8736	3.6567	3.7713	3.6075	3.1740
	10	3.7674	3.9998	3.7331	3.8595	3.6861	3.2333

Table 8 Non-dimensional natural frequency for SSSS Type-E1 rhombic plate (*a/h*=10)

Ξ^0	*n*	2-1-2	2-1-1	1-1-1	2-2-1	1-2-1	1-8-1
				CT-Type-E1			
15°	0.5	2.0671	1.7683	2.0597	1.4507	2.0462	1.9771
	1	2.0713	1.8395	2.0543	1.5974	2.0318	1.9212
	5	2.0742	1.8557	2.0359	2.0071	2.0020	1.7881
	10	2.0725	1.8533	2.0391	1.9945	2.0013	1.7593
30°	0.5	2.4400	2.1235	2.4305	1.6992	2.4133	2.3320
	1	2.4428	2.2142	2.4213	1.8939	2.3924	2.2628
	5	2.4382	2.2325	2.3903	2.3564	2.3457	2.1007
	10	2.4356	2.2298	2.3915	2.3390	2.3414	2.0658
45°	0.5	3.3184	2.0059	3.3014	2.2913	3.2742	3.1638
	1	3.3177	2.9264	3.2806	2.5781	3.2344	3.0606
	5	3.2930	3.0815	3.2143	3.1729	3.1420	2.8297
	10	3.2880	3.0775	3.2108	3.1423	3.1289	2.7815
60°	0.5	3.8917	1.6116	3.7479	3.2741	3.6569	3.4693
	1	3.9830	2.4897	3.7966	4.3292	3.6283	3.3715
	5	4.5086	2.7123	3.8884	4.1254	3.8158	3.3048
	10	4.5672	2.7030	4.0322	4.1839	3.9528	3.2797
				MT-Type-E1			
15°	0.5	1.0570	1.0534	1.0610	1.0463	1.0428	1.1128
	1	1.0596	1.0507	1.0683	1.1019	1.0685	1.3052
	5	1.0646	1.0528	1.0719	1.1484	1.1341	1.4992
	10	1.0650	1.0539	1.0946	1.1726	1.2104	1.6151
30°	0.5	1.2540	1.2481	1.2592	1.2411	1.1998	1.3216
	1	1.2571	1.2441	1.2657	1.3068	1.2697	1.5395
	5	1.2631	1.2448	1.2748	1.3629	1.3424	1.7804
	10	1.2635	1.2459	1.3006	1.3922	1.4404	1.9169
45°	0.5	1.7280	1.7139	1.3160	1.7066	1.5518	1.8263
	1	1.7330	1.7068	1.5623	1.8011	1.7555	2.1333
	5	1.7423	1.7040	1.7646	1.8820	1.8308	2.4610
	10	1.7430	1.7053	1.7991	1.9238	1.9966	2.6467
60°	0.5	1.6478	2.4330	1.0678	2.8000	2.1202	1.8758
	1	1.8577	2.5053	2.4321	2.7239	2.5023	2.3925
	5	2.8922	2.7390	3.1036	3.3015	2.8475	4.3233
	10	3.0461	2.7790	3.1650	3.3787	3.5248	4.5654

Tables 7, 8 show the value of non-dimensional natural frequency for Type- E and E1 simply supported rhombic plates, respectively (*a/h*=10). Skew angles of 15, 30,45,60 degrees are adopted in this study. With an increase in the value of the plate's skew angle, $\bar{\lambda}$ increases for all the cases.

5. Conclusions

In the present work free vibration response of FGSP is found by employing a zig-zag theory. The present model satisfies interlaminar stress continuity and is free from any post processing technique. FEM used for solving FGSP in the present study consists of nine-noded C-0 FE having 8DOF/node. Several new results are reported in the study which will serve as benchmark for future work in parallel direction. Following points are noted down in this study:
  • The boundary conditions, along with the thickness schemes, affect the vibration response of the plate.
  • With increase in thickness of core, value of non-dimensional natural frequency ($\bar{\lambda}$) increases for H-Type-E plate and decreases for S-Type-E plate.
  • Among Type-E, and E1 plates, the CT-Type-E1 plate gives the maximum value of $\bar{\lambda}$, and the MT-Type-E1 plate gives the least value of $\bar{\lambda}$.
  • With an increase in the value of the plate's skew angle, $\bar{\lambda}$ increases for all the cases.

Acknowledgments

References

Al-Fatlawi, A., Jarmai, K. and Kovacs, G. (2021), "Optimal design of a lightweight composite sandwich plate used for airplane containers", *Struct. Eng. Mech.*, **78**(5), 611-622. https://doi.org/10.12989/sem.2021.78.5.611.

Anderson, T.A. (2003), "A 3-D elasticity solution for a sandwich composite with functionally graded core subjected to transverse loading by a rigid sphere", *Compos. Struct.*, **60**(3), 265-274. https://doi.org/10.1016/S0263-8223(03)00013-8.

Antony, S., Cherouat, A. and Montay, G. (2019), "Hemp fibre woven fabric /polypropylene based honeycomb sandwich structure for aerospace applications", *Adv. Aircraft Spacecraft Sci.*, **6**(2), 87-103. https://doi.org/10.12989/aas.2019.6.2.087.

Averill, R.C. (1994), "Static and dynamic response of moderately thick laminated beams with damage", *Compos. Eng. J.*, **4**, 381-395. https://doi.org/10.1016/S0961-9526(09)80013-0.

Belabed, Z., Bousahla, A.A., Houari, M.S.A., Tounsi, A. and Mahmoud, S.R. (2018), "A new 3-unknown hyperbolic shear deformation theory for vibration of functionally graded sandwich plate", *Earthq. Struct.*, **14**(2), 103-115. https://doi.org/10.12989/eas.2018.14.2.103.

Benferhat, R., Daouadji, T.H. and Abderezak, R. (2021), "Effect of porosity on fundamental frequencies of FGM sandwich plates", *Compos. Mater. Eng.*, **3**(1), 25-40. https://doi.org/10.12989/cme.2021.3.1.025.

Brischetto, S., Carrera, E. and Demasi, L. (2009), "Improved bending analysis of sandwich plates using a zig-zag function", *Compos. Struct.*, **89**(3), 408-415. https://doi.org/10.1016/j.compstruct.2008.09.001.

Carrera, E. (2003), "Historical review of zig-zag theories for multilayered plates and shells", *Appl. Mech.*

Rev., **56**(3), 287-308. https://doi.org/10.1115/1.1557614.

Carrera, E. (2004), "On the use of the Murakami's zig-zag function in the modeling of layered plates and shells", *Comput. Struct.*, **82**(7-8), 541-554. https://doi.org/10.1016/j.compstruc.2004.02.006.

Chakrabarti, A., Chalak, H.D., Iqbal, M.A. and Sheikh, A.H. (2011), "A new FE model based on higher order zigzag theory for the analysis of laminated sandwich beam with soft core", *Compos. Struct.*, **93**(2), 271-279. https://doi.org/10.1016/j.compstruct.2010.08.031.

Chakraverty, S. and Pradhan, K.K. (2014), "Free vibration of exponential functionally graded rectangular plates in thermal environment with general boundary conditions", *Aerosp. Sci. Technol.*, **36**, 132-156. https://doi.org/10.1016/j.ast.2014.04.005.

Chalak, H.D., Chakrabarti, A., Iqbal, M.A. and Sheikh, A. H. (2013), "Free vibration analysis of laminated soft core sandwich plates", *J. Vib. Acoust.*, **135**(1), 011013. https://doi.org/10.1115/1.4007262.

Chareonsuk, J. and Vessakosol, P. (2011), "Numerical solutions for functionally graded solids under thermal and mechanical loads using a high-order control volume finite element method", *Appl. Therm. Eng.*, **31**(2-3), 213-227. https://doi.org/10.1016/j.applthermaleng.2010.09.001.

Cho, Y.B. and Averill, R.C. (2000), "First order zigzag sub-laminate plate theory and finite element model for laminated composite and sandwich panels", *Compos. Struct.*, **50**, 1-15. https://doi.org/10.1016/S0263-8223(99)00063-X.

Demasi, L. (2008), "∞3 Hierarchy plate theories for thick and thin composite plates: the generalized unified formulation", *Compos. Struct.*, **84**(3), 256-270. https://doi.org/10.1016/j.compstruct.2007.08.004.

Di Sciuva, M. (1985), "Development of anisotropic multilayered shear deformable rectangular plate element", *Comput. Struct.*, **21**, 789-96. https://doi.org/10.1016/0045-7949(85)90155-5.

Di Sciuva, M. (1993), "A general quadrilateral multilayered plate element with continuous interlaminar stresses", *Comput. Struct.*, **47**, 91-105. https://doi.org/10.1016/0045-7949(93)90282-I.

Ebrahimi, F. and Barati, M.R. (2017), "A third-order parabolic shear deformation beam theory for nonlocal vibration analysis of magneto-electro-elastic nanobeams embedded in two-parameter elastic foundation", *Adv. Nano Res.*, **59**(4), 313-336. https://doi.org/10.12989/anr.2017.5.4.313.

Ebrahimi, M.J. and Najafizadeh, M.M. (2014), "Free vibration analysis of two-dimensional functionally graded cylindrical shells", *Appl. Math Model.*, **38**(1), 308-324. https://doi.org/10.1016/j.apm.2013.06.015.

El-Galy, I.M., Bassiouny, I.S. and Mahmoud, H.A. (2019), "Functionally graded materials classifications and development trends from industrial point of view", *S.N. Appl. Sci.*, **1**(11), 1-23. https://doi.org/10.1007/s42452-019-1413-4.

Garg, A. and Chalak, H.D. (2019), "A review on analysis of laminated composite and sandwich structures under hygrothermal conditions", *Thin Wall. Struct.*, **142**, 205-226. https://doi.org/10.1016/j.tws.2019.05.005.

Garg, A., Belarbi, M.O., Chalak, H.D. and Chakrabarti, A. (2021), "A review of the analysis of sandwich FGM structures", *Compos. Struct.*, **258**, 113427. https://doi.org/10.1016/j.compstruct.2020.113427.

Garg, A., Chalak, H.D., Li, L., Belarbi, M.O., Sahoo, R. and Mukhopadhyay, T. (2022), "Vibration and buckling analyses of sandwich plates containing functionally graded metal foam core", *Acta Mechanica Solida Sinica*, 1-16. https://doi.org/10.1007/s10338-021-00295-z.

Hirane, H., Belarbi, M.O., Houari, M.S.A. and Tounsi, A. (2021), "On the layerwise finite element formulation for static and free vibration analysis of functionally graded sandwich plates", *Eng. Comput.*, 1-29. https://doi.org/10.1007/s00366-020-01250-1.

Khalafi, V. and Fazilati, J. (2021), "Free vibration analysis of functionally graded plates containing embedded curved cracks", *Struct. Eng. Mech.*, **79**(2), 157-168. https://doi.org/10.12989/sem.2021.79.2.157.

Koizumi, M. (1997), "FGM activities in Japan", *Compos. Part B*, **28**(1-2), 1-4. https://doi.org/10.1016/S1359-8368(96)00016-9.

Li, L. and Hu, Y. (2016), "Nonlinear bending and free vibration analyses of nonlocal strain gradient beams made of functionally graded material", *Int. J. Eng. Sci.*, **107**, 77-97. https://doi.org/10.1016/j.ijengsci.2016.07.011.

Meksi, R., Benyoucef, S., Mahmoudi, A., Tounsi, A., Adda Bedia, E.A. and Mahmoud, S.R. (2019), "An

analytical solution for bending, buckling and vibration responses of FGM sandwich plates", *J. Sandw. Struct. Mater.*, **21**(2), 727-757. https://doi.org/10.1177/1099636217698443.

Moleiro, F., Correia, V.F., Araújo, A.L., Soares, C.M., Ferreira, A.J.M. and Reddy, J.N. (2019), "Deformations and stresses of multilayered plates with embedded functionally graded material layers using a layerwise mixed model", *Compos. Part B: Eng.*, **156**, 274-291. https://doi.org/10.1016/j.compositesb.2018.08.095.

Murakami, H. (1986), "Laminated composite plate theory with improved in-plane responses.", *J. Appl. Mech.*, **53**(3), 661-666. https://doi.org/10.1115/1.3171828.

Neves, A.M.A., Ferreira, A.J., Carrera, E., Cinefra, M., Jorge, R.M.N. and Soares, C.M.M. (2012), "Static analysis of functionally graded sandwich plates according to a hyperbolic theory considering Zig-Zag and warping effects", *Adv. Eng. Softw.*, **52**, 30-43. https://doi.org/10.1016/j.advengsoft.2012.05.005.

Neves, A.M.A., Ferreira, A.J.M., Carrera, E., Cinefra, M., Jorge, R.M.N., Mota Soares, C.M. and Araújo, A.L. (2017), "Influence of zig-zag and warping effects on buckling of functionally graded sandwich plates according to sinusoidal shear deformation theories", *Mech. Adv. Mater. Struct.*, **24**(5), 360-376. https://doi.org/10.1080/15376494.2016.1191095.

Nguyen, K., Thai, H.T. and Vo, T. (2015), "A refined higher-order shear deformation theory for bending, vibration and buckling analysis of functionally graded sandwich plates", *Steel Compos. Struct.*, **18**(1), 91-120. https://doi.org/10.12989/scs.2015.18.1.091.

Owoputi, A.O., Inambao, F.L. and Ebhota, W.S. (2018), "A review of functionally graded materials: fabrication processes and applications", *Int. J. Appl. Eng. Res.*, **13**(23), 16141-16151.

Pandey, S. and Pradyumna, S. (2018), "Analysis of functionally graded sandwich plates using a higher-order layerwise theory", *Compos. Part B: Eng.*, **153**, 325-336. https://doi.org/10.1016/j.compositesb.2018.08.121.

Reddy, J. (2000), "Analysis of functionally graded plates", *Int. J. Numer. Meth. Eng.*, **47**(1-3), 663-684. https://doi.org/10.1002/(SICI)1097-0207(20000110/30)47:1/3<663::AID-NME787>3.0.CO;2-8.

Sahouane, A., Hadji, L. and Bourada, M. (2019), "Numerical analysis for free vibration of functionally graded beams using an original HSDBT", *Earthq. Struct.*, **17**(1), 31-37. https://doi.org/10.12989/eas.2019.17.1.031.

Shariyat, M. and Alipour, M.M. (2015), "Novel layerwise shear correction factors for zigzag theories of circular sandwich plates with functionally graded layers", *Lat. Am. J. Solid. Struct.*, **12**(7), 1362-1396. https://doi.org/10.1590/1679-78251477.

Sharma, R., Jadon, V. and Singh, B. (2015), "A review on the finite element methods for heat conduction in functionally graded materials", *J. Inst. Eng.*, **96**(1), 73-81. https://doi.org/10.1007/s40032-014-0125-1.

Swaminathan, K., Naveenkumar, D.T., Zenkour, A.M. and Carrera, E. (2015), "Stress, vibration and buckling analyses of FGM plates-A state-of-the-art review", *Compos. Struct.*, **120**, 10-31. https://doi.org/10.1016/j.compstruct.2014.09.070.

Tounsi, A., Houari, M.S.A. and Bessaim, A. (2016), "A new 3-unknowns non-polynomial plate theory for buckling and vibration of functionally graded sandwich plate", *Struct. Eng. Mech.*, **60**(4), 547-565. https://doi.org/10.12989/sem.2016.60.4.547.

Vel, S.S. and Batra, R. (2004), "Three-dimensional exact solution for the vibration of functionally graded rectangular plates", *J. Sound Vib.*, **272**(3-5), 703-730. https://doi.org/10.1016/S0022-460X(03)00412-7.

Woodward, B. and Kashtalyan, M. (2010), "Bending response of sandwich panels with graded core: 3D elasticity analysis", *Mech. Adv. Mater. Struct.*, **17**(8), 586-594. https://doi.org/10.1080/15376494.2010.517728.

Zenkour, A.M. (2005), "A comprehensive analysis of functionally graded sandwich plates: Part 1-Deflection and stresses", *Int. J. Solid. Struct.*, **42**(18-19), 5224-5242. https://doi.org/10.1016/j.ijsolstr.2005.02.015.

Zenkour, A.M. (2005), "A comprehensive analysis of functionally graded sandwich plates: Part 2-Buckling and free vibration", *Int. J. Solid. Struct.*, **42**(18-19), 5243-5258. https://doi.org/10.1016/j.ijsolstr.2005.02.016.

CC